LETTER

doi:10.1038/nature12992

Prodigious degassing of a billion years of accumulated radiogenic helium at Yellowstone

J. B. Lowenstern[1], W. C. Evans[1], D. Bergfeld[1] & A. G. Hunt[2]

Helium is used as a critical tracer throughout the Earth sciences, where its relatively simple isotopic systematics is used to trace degassing from the mantle, to date groundwater and to time the rise of continents[1]. The hydrothermal system at Yellowstone National Park is famous for its high helium-3/helium-4 isotope ratio, commonly cited as evidence for a deep mantle source for the Yellowstone hotspot[2]. However, much of the helium emitted from this region is actually radiogenic helium-4 produced within the crust by α-decay of uranium and thorium. Here we show, by combining gas emission rates with chemistry and isotopic analyses, that crustal helium-4 emission rates from Yellowstone exceed (by orders of magnitude) any conceivable rate of generation within the crust. It seems that helium has accumulated for (at least) many hundreds of millions of years in Archaean (more than 2.5 billion years old) cratonic rocks beneath Yellowstone, only to be liberated over the past two million years by intense crustal metamorphism induced by the Yellowstone hotspot. Our results demonstrate the extremes in variability of crustal helium efflux on geologic timescales and imply crustal-scale open-system behaviour of helium in tectonically and magmatically active regions.

Despite its notable mobility, the light element He can be stored over geologically extensive periods[3]. It is found in considerable quantities in some natural-gas reservoirs, where it remains stored for millions of years[3,4]. Yet it can rapidly traverse the crust in tectonically active regions where mantle ^{3}He leaks to the surface[5]. Recognition of He accumulations within sedimentary basins and oil fields spurred considerable research to assess whether the He migrates during steady-state degassing of the entire crust, or during more transient dynamic episodes associated with increased heat flow or tectonism[3,6,7]. Tracking the magnitude of accumulation of He within crustal rocks themselves, and the rapidity with which He can be purged, has not yet been fully explored.

Studies of He flux from active tectonic and magmatic regions usually focus on the mantle-derived component; those that include crustal flux have typically explored point sources limited in extent[7,8]. The Yellowstone plateau volcanic field is often viewed as a mantle hotspot with well-known high ^{3}He/^{4}He ratio (R) in gas from fumarolic vents and hot-spring waters[2,9]. Decades ago, workers recognized that Yellowstone's mantle He signature is diluted considerably by crustal ^{4}He, but at that time the mass flux of ^{4}He implied by this dilution was not appreciated.

Over the past ten years, we have combined studies of gas and isotope chemistry with measurements of CO_2 emission rates from thermal areas across Yellowstone National Park[10–13]. One clear result has been that the very high CO_2 emissions require considerable efflux of He. Gas emissions are concentrated in and around the Yellowstone caldera, which was formed during the last major caldera-forming eruption, 640 kyr ago. The caldera is the geographic focus for continuing uplift–subsidence cycles[14], presumably because its location coincides with the present-day input ($>0.1\,km^3\,yr^{-1}$) of mantle basalt into the crust[15,16]. The inferred mantle input is consistent with ^{3}He/^{4}He ratios (Fig. 1) that reach values more than sixteen times the atmospheric ratio (that is, $16R_a$) within the caldera. However, much lower values prevail in some parts of the caldera and the surrounding volcanic field.

Notably, ^{3}He/^{4}He ratios in gas from fumaroles and bubbling pools decrease as He concentrations increase (Fig. 2a). This is consistent with dilution of the mantle He signature by radiogenic crustal ^{4}He. Reduced R/R_a and increased He concentrations also correlate with increasing CH_4 and decreasing $\delta^{13}C$ CH_4 (Fig. 2), which are clear signs of crustal input[8]. ($\delta^{13}C$ (‰) $= [(^{13}C/^{12}C)_{sample}/(^{13}C/^{12}C)_{standard} - 1] \times 1{,}000$, where the standard is PeeDee Belemnite. The reference to CH_4 reflects that we are measuring the carbon isotopic ratio in CH_4.)

All these trends reflect in part the influence of Eocene Absaroka Supergroup rocks, which are present in the eastern part of the park and contribute gas with high ethane/methane ratios, low $\delta^{13}C$ CH_4 values and greater methane concentrations than are found in the rest of Yellowstone[10,17]. But the trends hold for all of Yellowstone up to the highest measured R/R_a values, supporting the interpretation that crustal ^{4}He input is the main reason all R/R_a values fall below the value of 22 inferred for the Yellowstone hotspot endmember[18].

At Yellowstone, the highest He concentrations yet found come from the Heart Lake Geyser Basin[12], at the south boundary of the caldera, adjacent to the active East Mount Sheridan faults that expose Palaeozoic metasediments. Reported He/CO_2, R/R_a, and CO_2 emissions[12] (Extended Data Figs 1 and 2) permit estimation of the crustal He flux from the geyser basin:

$$q^{C}_{He} = 3.65 \times 10^{8} \frac{Q_{CO_2}}{M_{CO_2}} \phi \frac{X_{He}}{X_{CO_2}}$$

where Q_{CO_2} is the measured emission of CO_2 in tonnes per day, M_{CO_2} is the molecular weight of CO_2, X_{He}/X_{CO_2} is the molar ratio and ϕ is the fraction of crustal He in the sample (Methods). The expression yields q^{C}_{He} in moles per year.

Calculated total He emissions from the Heart Lake Geyser Basin are $6{,}900\,mol\,yr^{-1}$ (Table 1). Given the very low R/R_a of gas samples from the Heart Lake area (1.1 to 2.9), and the presumed high R/R_a of the hotspot endmember (22), q^{C}_{He} is equal to $5{,}970\,mol\,yr^{-1}$ of crustal ^{4}He.

The rate of ^{4}He production due to α-decay of U and Th in the entire crust beneath Yellowstone (Q^{C}_{He} in moles per year) is equivalent to

$$Q^{C}_{He} = \frac{M_Y}{N_A}\alpha$$

where M_Y is the mass of the crust beneath Yellowstone in grams, N_A is Avogadro's constant and α is the crustal production of ^{4}He in atoms per gram per year. In turn

$$\alpha = 3.115 \times 10^{6}[U] + 1.272 \times 10^{5}[U] + 7.710 \times 10^{5}[Th]$$

where [U] and [Th] are respectively the concentrations of U (^{235}U and ^{238}U, hence the two terms) and Th in the crust in parts per million by weight[19]. Assuming an average crustal composition[20] and a 43-km-thick crust (Methods), the production rate of ^{4}He beneath Yellowstone is $17{,}100\,mol\,yr^{-1}$. The crustal ^{4}He flux from the 0.8-km^2 Heart Lake Geyser Basin is thus equivalent to ~35% of this whole-crust (WC) production rate beneath the 9,000-km^2 park.

[1]US Geological Survey, Menlo Park, California 94025, USA. [2]US Geological Survey, Denver, Colorado 80225, USA.

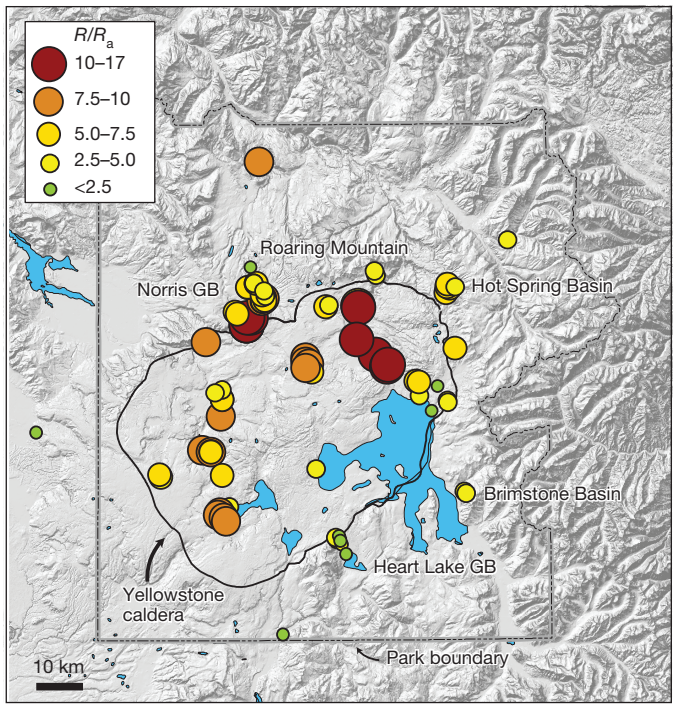

Figure 1 | Map of Yellowstone. Circles denote sample locations colour-coded and sized by He isotope composition (R/R_a) as depicted in the key (all values were corrected for minor air contamination). Thermal areas discussed in the text are shown; the relevant samples are immediately to the left of the area name, except for Norris Geyser Basin (to right). Data are from refs 10, 16.

Other degassing areas around the periphery of the caldera also have very low R/R_a owing to evident addition of crustal He (refs 9, 10 and 18). Combining annual estimated emissions for Hot Spring Basin[11], Brimstone Basin[13] and Roaring Mountain[16] with Heart Lake Geyser Basin yields the equivalent of 28WC (Table 1). Yet these four locations, which have a combined area of ~5 km^2, represent <10% of the total heat[21] and gas[16] flux at Yellowstone. We also estimate the total radiogenic He flux from the entire Yellowstone hydrothermal system. The median air-corrected R/R_a of gas from 83 localities within and outside the caldera is 6.9 (Extended Data Fig. 1), which is far less than the value for the hotspot endmember[18], of 22. Our best park-wide estimate of crustal ^{4}He flux is 597WC, or 21 times greater than the four thermal areas estimated above.

It is possible that some of the trend in Fig. 2a could be due to a second mantle endmember such as very old subcontinental lithospheric mantle with $^3He/^4He = 4R_a–6R_a$, which is thought by many to be an important magma source in Snake River Plain magmatism[22]. Involvement of subcontinental lithospheric mantle would not explain the observed trends in CH_4/CO_2 or $\delta^{13}C$ CH_4 versus R/R_a (Fig. 2), nor the higher NH_3 concentration and C_2H_6/CH_4 in gases with low R/R_a (ref. 10). Methane and C_2H_6 are normally produced at temperatures less than 300 °C and by thermogenesis from organic sediments, and are unstable in high-temperature, mantle-derived volcanic gas[23]. Nevertheless, we calculate crustal ^{4}He fluxes assuming both the Yellowstone hotspot endmember, with $R = 22R_a$ (ref. 18), as well as a bulk mixed mantle with $R = 11R_a$ (Table 1). This value represents the lowest $^3He/^4He$ ratio found in a suite of basalt-hosted olivines from nine localities throughout the eastern Snake River Plain[22]. Using both mantle endmembers, we constrain the total crustal ^{4}He emissions from Yellowstone at between 86WC and 1,970WC, with a best estimate of 597WC. If the whole crust beneath Yellowstone were particularly U- and Th-rich (4 parts U per million and 12 parts Th per million), this would decrease to 238WC. Degassing of the Yellowstone hydrothermal system thus yields tens to hundreds of times more radiogenic He than can be supported by the underlying crust. If similar He emissions were discharged over the 2-Myr history of the Yellowstone plateau volcanic field, then between 172 and 3,940 Myr of accumulated radiogenic He must have been emitted during that time (best estimate of 1,194 Myr).

Such great volumes of He would be particularly difficult to explain if the crust were composed entirely of young volcanic rock. Though Pleistocene volcanic rocks crop out at the surface in the caldera, and Eocene rocks of the Absaroka Supergroup dominate at the park's

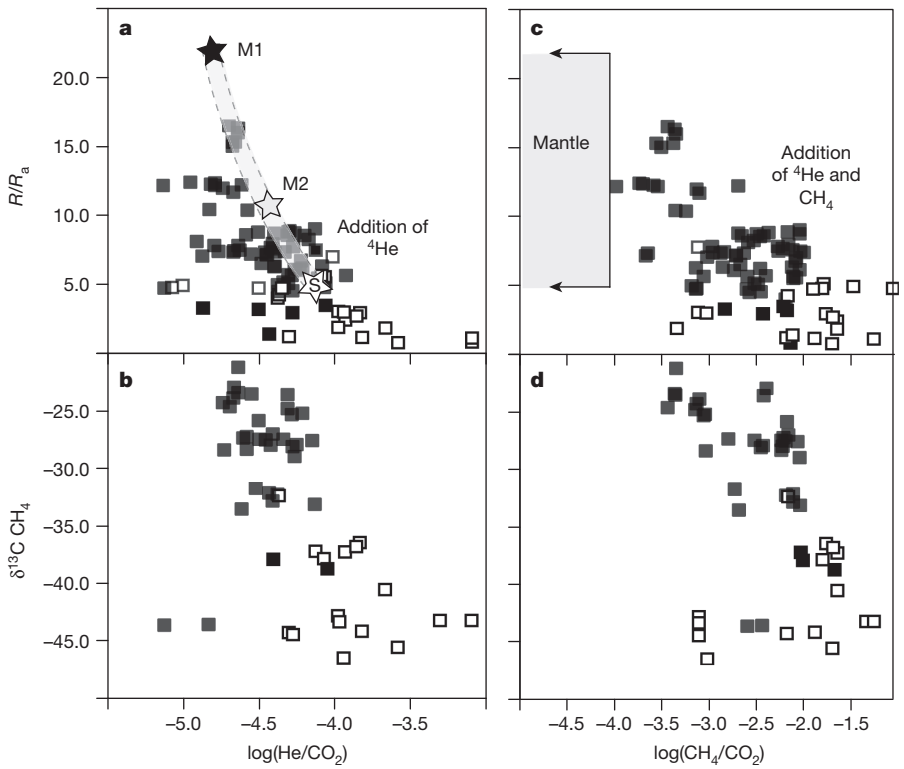

Figure 2 | Concentration and isotope ratios for Yellowstone gases. **a**, $^3He/^4He$ (as R/R_a) versus $\log(He/CO_2)$; **b**, $\delta^{13}C$ CH_4 versus $\log(He/CO_2)$; **c**, $^3He/^4He$ (as R/R_a) versus $\log(CH_4/CO_2)$; **d**, $\delta^{13}C$ CH_4 versus $\log(CH_4/CO_2)$. CO_2 makes up >90% of virtually all Yellowstone gas samples (steam excluded). Open squares show the extracaldera thermal areas denoted in Fig. 1 plus those clearly emerging through Absaroka volcaniclastic rocks at the caldera's eastern edge. Filled squares are intracaldera thermal features plus those of the adjacent Norris Geyser Basin. In **a**, mantle endmembers M1 (ref. 18) and S (ref. 22) (subcontinental lithospheric mantle) are mixed along the grey bar to create M2, which is used along with M1 in flux calculations (Methods). Locations of M1, M2 and S in **b**–**d** are unknown, although $\log(CH_4/CO_2)$ should be less than −4.0 in high-temperature, mantle-derived gas[23], and if CH_4 were present then $\delta^{13}C$ CH_4 would be above −25. Errors for Yellowstone gases are smaller than the symbol size. Data are from ref. 10.

Table 1 | CO_2, He and radiogenic He flux for Yellowstone and select thermal areas

Region	Q_{CO_2} (t d^{-1})	Q_{He} (mol yr^{-1})	R/R_a	$q^C_{He}(1)$ (mol yr^{-1})	$q^C_{He}(2)$ (mol yr^{-1})	WC(1)	WC(2)
Heart Lake Basin	6	6.91×10^3	3.0	5.97×10^3	5.03×10^3	0.35	0.29
Brimstone Basin	277	2.50×10^5	3.0	2.16×10^5	1.82×10^5	12.6	10.6
Hot Spring Basin	410	2.39×10^5	5.5	1.79×10^5	1.19×10^5	10.5	7.0
Roaring Mountain	100	8.49×10^4	1.9	7.77×10^4	7.05×10^4	4.5	4.1
Entire park (min)	20,000	3.95×10^6	6.9	2.71×10^6	1.47×10^6	159	86.2
Entire park (max)	80,000	4.92×10^7	6.9	3.38×10^7	1.83×10^7	1,970	1,070
Entire park (best)	45,000	1.49×10^7	6.9	1.02×10^7	5.55×10^6	597	324

$q^C_{He}(1)$ is the crustal He flux assuming a mantle R/R_a of 22. $q^C_{He}(2)$ is the crustal He flux assuming a mantle R/R_a of 11. WC(1) and WC(2) are the two corresponding calculated crustal ^{4}He fluxes relative to the ^{4}He annually produced by a 43-km-thick crustal section (9,000 km^2). See the Supplementary Information for the source data for Table 1.

eastern edge, older rocks almost certainly make up the mid to lower crust that hosts the intrusive complex feeding the surface volcanism[24]. Yellowstone sits astride the Wyoming craton near the northeast–southwest-trending boundary between two of its subdivisions, the Montana sedimentary province and the Beartooth–Bighorn magmatic zone[25]. The former has rocks as old as 3.5 Gyr with detrital zircons as old as 4.0 Gyr. Early Yellowstone rhyolites inherited a strong isotope signature (in Sr, Nd and Pb) from this old crust, implying that the rhyolites were formed through hybridization of fractionates of mantle-derived basalts with melts of crustal Archaean rock[26]. More recent volcanism, particularly within the caldera, indicates less input from old crust, because this fertile source wanes in abundance and new magma is generated by recycling of hydrothermally altered volcanic rocks and fractionation of the existing magma reservoir[24,26,27]. Only outside the caldera margins does a strong Archaean signature remain[26]. Similarly, it is likely that early magmatism caused greater amounts of crustal degassing within the caldera, and that the present measured flux of crustal ^{4}He is somewhat reduced relative to the initial stages of volcanism.

Numerous studies indicate that this part of the Wyoming craton was stabilized by 2.8 Gyr ago and since then has undergone relatively little tectonism until the present day. Potassium–argon ages of ~2.3 Gyr from cratonic basement rocks imply that they stayed at a temperature of less than ~350 °C for more than 2 Gyr, and that development of a stable tectosphere and deep mantle root shielded the area from subsequent regional orogens[25,28]. Consequently, there has been relatively little potential to mobilize accumulated He.

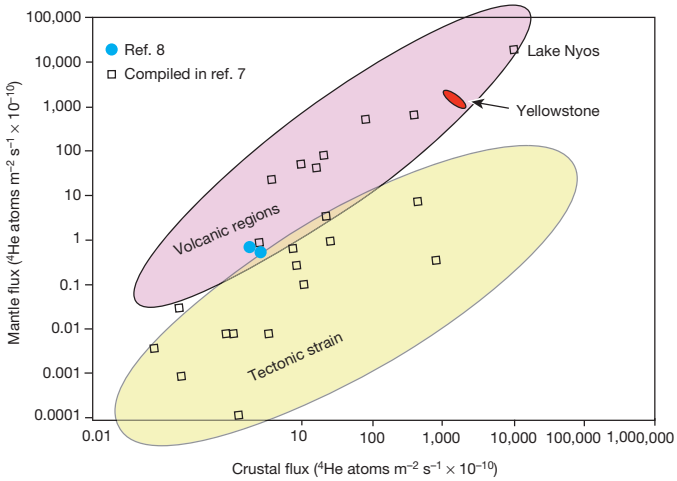

Figure 3 | Crustal versus mantle ^{4}He flux based on ref. 7. Data for the original diagram were modelled assuming that $R \approx 0.01R_a$ in the crust and $R = 8.6R_a$ in the mantle. Volcanic regions were found to release significantly more mantle He, but also frequently more crustal He, than non-volcanic areas. The Yellowstone data lie at the high-flux end of the volcanic field for both mantle and crustal He. Values for the Yellowstone field cover the region between the two mantle endmembers used in Table 1. Data from ref. 8 represent an early study using similar methods, but in a younger, less (volcanically) active crustal region. Lake Nyos is a small crater lake in Cameroon with abundant CO_2 discharge.

The elements U and Th, which dominate the production of radiogenic He in the crust[19], are located primarily in the mineral zircon and other accessory minerals such as monazite, titanite and apatite that are common in igneous and metamorphic rocks. Above a mineral's theoretical blocking temperature, an element of interest will diffuse out of the mineral and into the surrounding rocks. Helium should diffuse out of zircon and titanite at temperatures exceeding ~200 °C (ref. 29), as would occur at depths >10 km in all but the lowest of geothermal gradients. However, without a path for advective fluid flow in the host rocks, He cannot escape and will remain trapped in the very low-permeability rocks that reside in undisturbed (that is, tectonically unmodified) mid-to-lower crust[30]. Without significant fluid advection or large He concentration gradients, the rate of He diffusion is simply too slow to allow for He migration on crustal timescales[19].

Examples of long-term He residence in the crust are reported increasingly often. Recently, Archaean waters were identified in fractures in a mine from the Precambrian Shield of Ontario[31]. A residence time of 1.1 ± 0.6 Gyr was calculated for He in this fluid. In many rocks, fluid inclusions are ideal receptacles for He (ref. 32), which partitions strongly into any gas bubble relative to the host mineral: fluid inclusions in the Archaean Witwatersrand Basin, in South Africa, retained their initial trapped Ne for much more than 2 Gyr (ref. 33). And over the past few decades, workers have become increasingly convinced that both mantle and radiogenic He can accumulate over geological time within crustal aquifers and gas reservoirs[3,4,6,7,19].

Never before, though, has non-steady-state emission of radiogenic gas been so clearly illustrated. Over the past 2 Myr, the Yellowstone hotspot has penetrated one of the oldest cratons on the planet, resulting in tectonic strain, fracturing, melting and infiltration by circulating metamorphic and hydrothermal fluids. About 50% of our samples have $CO_2/^3$He ratios between 2×10^9 and 4×10^9, implying that a consistent mantle signature for CO_2 is present throughout the region. The mantle-derived gas flux scavenges any crustal ^{4}He made increasingly available through the tectonic and metamorphic processes noted above. A recent compilation of values for crustal He flux noted increased crustal and mantle He flux in volcanic regions[7], relative to non-volcanic terrains, but the data set was largely limited to crater lakes a few square kilometres in size and for time periods of years to decades. Our Yellowstone results fall on the upper part of this trend and greatly expand the spatial and temporal scales (Fig. 3).

Noble-gas data are frequently interpreted by assuming closed systems, where circulating fluids interact solely with rocks and sediments of local aquifers. More rapid addition of crustal ^{4}He implies that mean groundwater transit times can be orders of magnitude shorter than those calculated on the basis of closed-system assumptions. Our work demonstrates that open-system behaviour can dominate noble-gas budgets in regions of active magmatism and tectonics. Yet it also demonstrates an example of closed-system behaviour within a stable Archaean craton, where He initially accumulated for billions of years before incursion of the Yellowstone hotspot.

METHODS SUMMARY

Gas samples were collected from fumaroles and hot springs in evacuated, NaOH-bearing glass bottles according to standard methods[10]. Diffuse CO_2 flux was estimated by the accumulation chamber technique[11–13,16]. Gas chemistry was determined with a

combination of gas chromatography, ion chromatograph and manometry[10] in the geothermal laboratory in Menlo Park, California. Noble-gas isotopic ratios, including those for He, were measured in Denver, Colorado, at the USGS Noble Gas Laboratory. A detailed description of the methods and further information about the assumptions used in our calculations are provided in Methods.

Online Content Any additional Methods, Extended Data display items and Source Data are available in the online version of the paper; references unique to these sections appear only in the online paper.

Received 15 August; accepted 11 December 2013.

1. Porcelli, D., Ballentine, C. J. & Wieler, R. *Noble Gases in Geochemistry and Cosmochemistry* (Rev. Mineral. Geochem. 47, Mineralogical Society of America and the Geochemical Society, 2002).
2. Craig, H., Lupton, J. E., Welhan, J. A. & Poreda, R. Helium isotope ratios in Yellowstone and Lassen Park volcanic gases. *Geophys. Res. Lett.* **5,** 897–900 (1978).
3. Ballentine, C. J., Burgess, R. & Marty, B. Tracing fluid origin, transport and interaction in the crust. *Rev. Mineral. Geochem.* **47,** 539–614 (2002).
4. Ballentine, C. J. & Sherwood Lollar, B. Regional groundwater focusing of nitrogen and noble gases in the Hugoton-Panhandle giant gas field, USA. *Geochim. Cosmochim. Acta* **66,** 2483–2497 (2002).
5. Kennedy, B. M. *et al.* Mantle fluids in the San Andreas fault system, California. *Science* **278,** 1278–1281 (1997).
6. Torgersen, T. & Clarke, W. B. Helium accumulation in groundwater, I: an evaluation of sources and the continental flux of crustal ^{4}He in the Great Artesian Basin, Australia. *Geochim. Cosmochim. Acta* **49,** 1211–1218 (1985).
7. Torgersen, T. Continental degassing flux of ^{4}He and its variability. *Geochem. Geophys. Geosyst.* **11,** Q06002 (2010).
8. Sano, Y., Wakita, H. & Huang, C.-W. Helium flux in a continental land area estimated from ^{3}He/^{4}He ratio in northern Taiwan. *Nature* **323,** 55–57 (1986).
9. Kennedy, B. M., Lynch, M. A., Reynolds, J. H. & Smith, S. P. Intensive sampling of noble gases in fluids at Yellowstone, I. Early overview of the data; regional patterns. *Geochim. Cosmochim. Acta* **49,** 1251–1261 (1985).
10. Bergfeld, D. B. *et al. Gas and Isotope Chemistry of Thermal Features in Yellowstone National Park, Wyoming*. Scientific Investigations Report 2011–5012 (US Geological Survey, 2011).
11. Werner, C. *et al.* Volatile emissions and gas geochemistry of Hot Spring Basin, Yellowstone National Park, USA. *J. Volcanol. Geotherm. Res.* **178,** 751–762 (2008).
12. Lowenstern, J. B., Bergfeld, D., Evans, W. C. & Hurwitz, S. Generation and evolution of hydrothermal fluids at Yellowstone: insights from the Heart Lake Geyser Basin. *Geochem. Geophys. Geosyst.* **13,** Q01017 (2012).
13. Bergfeld, D. B., Evans, W. C., Lowenstern, J. B. & Hurwitz, S. Carbon dioxide and hydrogen sulfide degassing and cryptic thermal input to Brimstone Basin, Yellowstone National park, Wyoming. *Chem. Geol.* **330–331,** 233–243 (2012).
14. Smith, R. B. *et al.* Geodynamics of the Yellowstone hotspot and mantle plume: Seismic and GPS imaging, kinematics, and mantle flow. *J. Volcanol. Geotherm. Res.* **188,** 26–56 (2009).
15. Lowenstern, J. B. & Hurwitz, S. Monitoring a supervolcano in repose: heat and volatile flux at the Yellowstone Caldera. *Elements* **4,** 35–40 (2008).
16. Werner, C. & Brantley, S. CO_2 emissions from the Yellowstone volcanic system. *Geochem. Geophys. Geosyst.* **4,** 1061 (2003).
17. Lorenson, T. D. & Kvenvolden, K. A. in *The Future of Energy Gases* (eds Howell D. G. *et al.*) 453–470 (Profession Paper 1570, US Geological Survey, 1993).
18. Chiodini, G. *et al.* Insights from fumarole gas geochemistry on the origin of hydrothermal fluids on the Yellowstone Plateau. *Geochim. Cosmochim. Acta* **89,** 265–278 (2012).
19. Ballentine, C. J. & Burnard, P. G. Production, release and transport of noble gases in the continental crust. *Rev. Mineral. Geochem.* **47,** 481–538 (2002).
20. Rudnick, R. & Fountain, D. M. Nature and composition of the continental crust: a lower crustal perspective. *Rev. Geophys.* **33,** 267–309 (1995).
21. Vaughan, R. G., Keszthelyi, L. P., Lowenstern, J. B., Jaworowski, C. & Heasler, H. Use of ASTER and MODIS thermal infrared data to quantify heat flow and hydrothermal change at Yellowstone National Park. *J. Volcanol. Geotherm. Res.* **233–234,** 72–89 (2012).
22. Graham, D. W. *et al.* Mantle source provinces beneath the Northwestern USA delimited by helium isotopes in young basalts. *J. Volcanol. Geotherm. Res.* **188,** 128–140 (2009).
23. Chiodini, G. CO_2/CH_4 ratio in fumaroles a powerful tool to detect magma degassing at quiescent volcanoes. *Geophys. Res. Lett.* **36,** L02302 (2009).
24. Christiansen, R. L. *The Quaternary and Pliocene Yellowstone Plateau Volcanic Field of Wyoming, Idaho, and Montana.* Professional Paper 729-G (US Geological Survey, 2001).
25. Mueller, P. & Frost, C. The Wyoming Province: a distinctive Archean craton in Laurentian North America. *Can. J. Earth Sci.* **43,** 1391–1397 (2006).
26. Hildreth, W., Halliday, A. N. & Christiansen, R. L. Isotopic and chemical evidence concerning the genesis and contamination of basaltic and rhyolitic magma beneath the Yellowstone Plateau Volcanic Field. *J. Petrol.* **32,** 63–138 (1991).
27. Bindeman, I. N., Fu, B., Kita, N. T. & Valley, J. W. Origin and evolution of silicic magmatism at Yellowstone based on ion microprobe analysis of isotopically zoned zircons. *J. Petrol.* **49,** 163–193 (2008).
28. Mueller, P. A., Mogk, D. W., Henry, D. J., Wooden, J. L. & Foster, D. A. Geologic evolution of the Beartooth Mountains: insights from petrology and geochemistry. *Northwest Geol.* **37,** 5–20 (2008).
29. Farley, K. A. (U-Th)/He dating: techniques, calibrations and applications. *Rev. Mineral. Geochem.* **47,** 819–844 (2002).
30. Ingebritsen, S. E. & Manning, C. E. Permeability of the continental crust: dynamic variations from seismicity and metamorphism. *Geofluids* **10,** 193–205 (2010).
31. Holland, G. *et al.* Deep fracture fluids isolated in the crust since the Precambrian era. *Nature* **497,** 357–360 (2013).
32. Sapienza, G., Hilton, D. R. & Scribano, V. Helium isotopes in peridotite mineral phases from Hyblean Plateau xenoliths (south-eastern Sicily, Italy). *Chem. Geol.* **219,** 115–129 (2005).
33. Lippmann-Pipke, J. *et al.* Neon identifies two billion year old fluid component in Kappvaal Craton. *Chem. Geol.* **283,** 287–296 (2011).

Supplementary Information is available in the online version of the paper.

Acknowledgements We thank S. Ingebritsen for a review. C. Hendrix, S. Gunther, H. Heasler and D. Mahony assisted with field planning and logistics.

Author Contributions J.B.L. and D.B. together led the sampling program at Yellowstone. W.C.E. participated in the fieldwork. D.B. did all laboratory analyses except the noble-gas analyses. D.B. also led the diffuse degassing fieldwork at Brimstone Basin and Heart Lake. A.G.H. performed the noble-gas analyses. J.B.L. first recognized the significance of the He emission rates for crustal degassing and wrote the first draft of the manuscript. W.C.E. provided considerable input on gas geochemistry and noble-gas systematics, and assisted with subsequent drafts. All authors edited later versions of the manuscript.

Author Information Reprints and permissions information is available at www.nature.com/reprints. The authors declare no competing financial interests. Readers are welcome to comment on the online version of the paper. Correspondence and requests for materials should be addressed to J.B.L. (jlwnstrn@usgs.gov).

METHODS

Gas sampling. Gas samples are collected from fumaroles and hot springs in evacuated, NaOH-bearing glass (Giggenbach) bottles according to standard methods. Full analytical details and the entire data set up to 2009 are provided in ref. 10. Data for samples used in Figs 1 and 2 including unpublished 2010 and 2011 analyses are provided with the Source Data for those figures. Gas chemistry is determined with a combination of gas chromatography, ion chromatograph and manometry in the geothermal laboratory in Menlo Park, California. Similar analyses of Yellowstone gas samples were reported in refs 16, 18 using facilities at other laboratories, yielding comparable results. Noble-gas isotopic ratios, including those for He, were measured in Denver, Colorado, at the USGS Noble Gas Laboratory.

Diffuse degassing estimates. Diffuse CO_2 flux in thermal areas is measured through standard accumulation chamber techniques[34]. The diffuse flux represents only a partial estimate of the total gas flux, because additional gas is emitted directly through vents such as fumaroles and bubbling pools. Vent emissions are estimated to represent 32 to 63% of the total degassing at Mud Volcano[35] (Yellowstone National Park).

R_a versus R_c. All calculations in Table 1 and all plots are based on R_c/R_a rather than R/R_a, where R_c represents $^3He/^4He$ corrected for minor air contamination determined through the He/Ne ratio and assuming all Ne to be atmosphere derived. These corrections are minimal: the median R_c/R_a for Yellowstone gases is 6.9, compared with 6.7 for R/R_a. This small variation has <1% effect on the crustal ^4He flux (q^C_{He}) for Yellowstone when using mantle endmember 1 ($22R_a$). The effect is greater when using mantle endmember 2 ($11R_a$), increasing q^C_{He} by 5% when the uncorrected values are used. The distribution of R_c/R_a at Yellowstone is shown in Extended Data Fig. 1.

CO_2/He. The CO_2/He ratios in our calculations come from fumaroles and bubbling pools rather than soil gas. Existing data confirm that CO_2/He is similar in soil gas and thermal features. Temporal variations in R/R_a and CO_2/He are minimal as indicated by the repeat sampling in ref. 10 and comparison with earlier noble-gas data sets such as that in ref. 9. We therefore expect that our samples are representative of present-day gas chemistry and isotopic compositions. The distribution of CO_2/He at Yellowstone is shown in Extended Data Fig. 2.

Mantle endmembers. Mantle endmember 1 (M1) is assumed to have a $^3He/^4He$ ratio of $22R_a$ (ref. 18). Assuming that $CO_2/^3He = 2 \times 10^9$ and $X_{CO_2} = 0.99$ fixes this gas at 16 p.p.m. He, or $\log(He/CO_2) = -4.8$ in Fig. 2a. Notwithstanding considerable past research on the Yellowstone system, there remains no clear indication of a second mantle gas source beneath Yellowstone[9,18], and we interpret the drop in R/R_a as being due to the influence of crust-derived gas.

Nevertheless, very old, low-R_a subcontinental mantle (SCLM) could supply abundant ^4He to Yellowstone gases and should be evaluated. If SCLM is present, it is difficult to identify because of the strong influence of atmosphere-derived gases produced by boiling of meteoric water at Yellowstone[9,10,18]. And if SCLM is present, its influence is minimal at locations such as Mud Volcano and Gibbon Geyser Basin (high-R_a samples on Fig. 1 south of Norris Geyser Basin).

At other locations, one way to estimate an alternative bulk mantle source that feeds gas through the Yellowstone crust is to examine olivine crystals in basalts from the Snake River Plain[22]. We select those samples with the lowest He isotope ratio ($11R_a$) as a justifiable endmember of samples that seem to be a mixture of hotspot and SCLM mantle endmembers[22]. We use this mixed mantle gas as the basis to calculate the second estimate of crustal ^4He flux (M2) listed in Table 1. We predict its He concentration by assuming that $CO_2/^3He = 2 \times 10^9$ and $R/R_a = 5$ (ref. 36), the concentration of He in the SCLM would then be 71 p.p.m., or $\log(He/CO_2) = -4.2$ (Fig. 2). We stress that even using a bulk mantle endmember of $8R_a$ (~50% SCLM of $5R_a$ and 50% M1 of $22R_a$) still results in $q^C_{He} > 100$WC. And, furthermore, if all mantle He was sourced from SCLM with $R_a = 5$ (ignoring those Yellowstone samples with higher R_a), Brimstone Basin, Heart Lake Geyser Basin and Roaring Mountain would still yield $q^C_{He} = 9$WC.

Crustal mixing. The proportion of crustal gas, ϕ, is calculated assuming a crustal endmember, $R_C = 0.01R_a$, and either of the two mantle endmembers, $R_M = 22R_a$ or $11R_a$. R_L represents the R/R_a of the local fluid at the individual thermal area, or the median for the Yellowstone hydrothermal system. Then

$$\phi = (R_M - R_L)/(R_M - R_C)$$

In Fig. 3, assuming a hotspot mantle endmember with $R_M = 22R_a$ yields 2,180 and 982 atoms $m^{-2}\,s^{-1} \times 10^{-10}$ for crustal and mantle ^4He, respectively. Assuming instead a mantle endmember with $R_M = 11R_a$ implies that more ^4He comes from the mantle, with 1,189 and 1,973 atoms $m^{-2}\,s^{-1} \times 10^{-10}$ from crust and mantle, respectively. These values are based on a total He flux of 1.49×10^7 mol yr^{-1} of He emitted from Yellowstone (Table 1).

Heart Lake Geyser Basin. The best estimate for CO_2 emissions is 6 t d^{-1} (ref. 12). The used CO_2/He ratio of 7,208 was the highest value at Heart Lake Geyser Basin, providing a conservative estimate of the total He flux (6,910 mol yr^{-1}). The used R_c/R_a of the local geothermal fluid of 3.0 also represents the highest value at Heart Lake Geyser Basin, where the thermal fluid first issues at the north end of the basin. Again, this provides a conservative estimate of the radiogenic He flux (5,030 mol yr^{-1}, assuming a mantle endmember with $R = 11R_a$ and 5,970 mol yr^{-1} for an endmember with $R = 22R_a$).

Hot Spring Basin. The best estimate for CO_2 emissions is 410 t d^{-1} (ref. 11). The used CO_2/He ratio of 14,218 was the median value from Hot Spring Basin ($n = 8$), yielding a He flux of (239,000 mol yr^{-1}). The R_c/R_a of the local geothermal fluid of 5.5 represents the median value at Hot Spring Basin ($n = 5$). Use of mean values provides similar estimates. The radiogenic He flux is 119,700 mol yr^{-1} assuming a mantle endmember with $R = 11R_a$ and 179,500 mol yr^{-1} for an endmember of $R = 22R_a$.

Brimstone Basin. The best estimate for CO_2 emissions is 277 t d^{-1} (ref. 13). The used CO_2/He ratio of 9,191 was the median value from Brimstone Basin, yielding a He flux of (250,000 mol yr^{-1}). The R_c/R_a of the local geothermal fluid of 3.0 also represents the median value at Brimstone Basin ($n = 3$). Use of mean values provides identical estimates. The radiogenic He flux is 182,000 mol yr^{-1} assuming a mantle endmember with $R = 11R_a$ and 216,000 mol yr^{-1} for an endmember with $R = 22R_a$.

Roaring Mountain. The best estimate for CO_2 emissions is 100 t d^{-1}, on the basis of data from ref. 16 and a conservative estimate of the area of the relevant region. The used CO_2/He ratio of 9,771 was the average value of two analyses, yielding a He flux of (85,000 mol yr^{-1}). The R_c/R_a of the local geothermal fluid is 1.9 ($n = 2$). The radiogenic He flux is 70,500 mol yr^{-1} assuming a mantle endmember with $R = 11R_a$ and 77,700 mol yr^{-1} for an endmember with $R = 22R_a$.

Yellowstone National Park. The best estimate for CO_2 emissions is 45,000 t d^{-1} (ref. 16), which is the estimated diffuse flux for Yellowstone, not including direct emanations from pools and fumaroles. We consider a minimum value of 20,000 t d^{-1} and a maximum of 80,000 t d^{-1}, the latter assuming that the vent flux makes up an additional 35,000 tonnes. Median, upper (25% quartile) and lower (75% quartile) estimates were calculated for molar CO_2/He; they are 25,100, 42,000 and 13,500, respectively. All calculations assumed the median R_c/R_a of 6.9 (the mean is nearly identical). Extended Data Figs 1 and 2 depict the range in values for both CO_2/He and R_c/R_a, including median, quartiles and 95% cutoffs. Replicate analyses of thermal features were averaged before calculating the statistics. Table 1 reports the minimum, maximum and 'best' estimate determined assuming mantle endmembers of both $R = 22R_a$ and $R = 11R_a$.

Crustal degassing estimates. The WC values represent radiogenic ^4He that can be produced in one year by a 43-km-thick crustal section, consistent with estimates for Archaean crust near Yellowstone[37]. The calculation includes the entire 9,000 km^2 of Yellowstone National Park. Crust is assumed to have a density of 3,000 kg m^{-3} and U and Th concentrations (1.4 and 5.6 p.p.m., respectively) appropriate for average continental crust[20]. The calculated ^4He yield for a gram of rock is equal to 8.86×10^6 atoms yr^{-1}. The yield for U-rich upper crust (12 p.p.m. Th and 4 p.p.m. U) would be 2.5 times higher, thus reducing our estimated WC values accordingly if the entire crust were anomalously U and Th rich.

34. Lewicki, J. L. *et al.* Comparative soil CO_2 flux measurements and geostatistical estimation methods on Masaya volcano, Nicaragua. *Bull. Volcanol.* **68,** 76–90 (2005).
35. Werner, C., Brantley, S. & Boomer, K. CO_2 emissions related to the Yellowstone volcanic system 2. Statistical sampling, total degassing, and transport mechanisms. *J. Geophys. Res.* **105,** 10831–10846 (2000).
36. Dunai, T. J. & Porcelli, D. Storage and transport of noble gases in the subcontinental lithosphere. *Rev. Mineral. Geochem.* **47,** 371–409 (2002).
37. Peng, X. & Humphreys, E. D. Crustal velocity structure across the eastern Snake River Plain and the Yellowstone swell. *J. Geophys. Res.* **103,** 7171–7186 (1998).

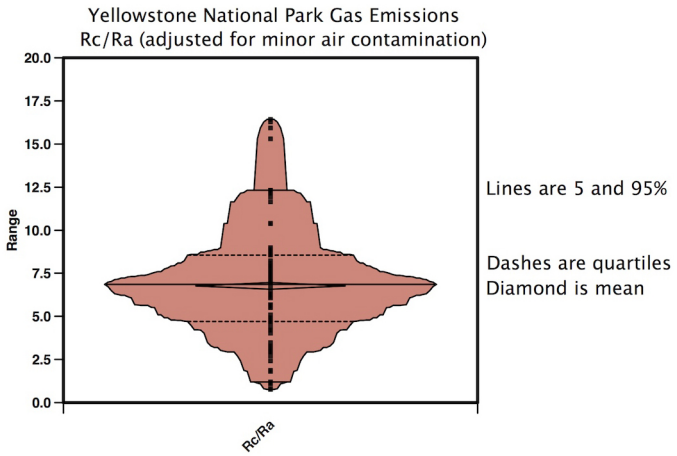

Extended Data Figure 1 | Box plot with distribution shape for R_c/R_a values from 83 locations in Yellowstone National Park after averaging multiple analyses from a single site. The dashed lines are the quartiles. The solid horizontal lines are respectively the 5th and 95th percentiles and the median. The short, broad diamond represents the mean and the black dots are individual data.

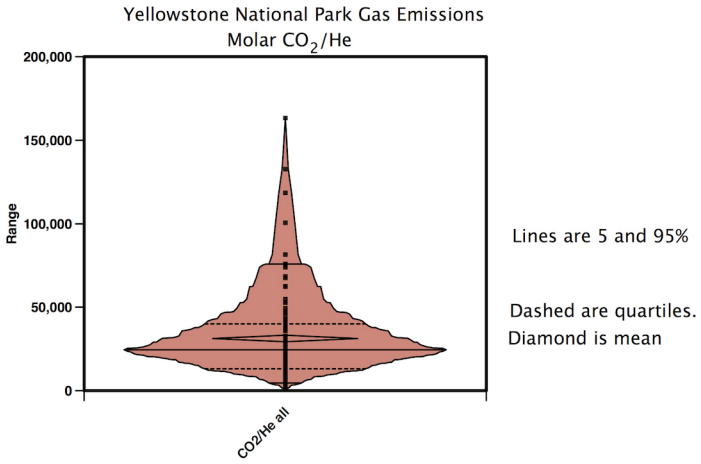

Extended Data Figure 2 | Box plot with distribution shape for CO_2/He in gas from 107 locations in Yellowstone National Park after averaging multiple analyses from a single site. The dashed lines are the quartiles. The solid horizontal lines are respectively the 5th and 95th percentiles and the median. The short, broad diamond represents the mean and the black dots are individual data.